Eddy-modulated, super-inertial turbulence

Robert B. Scott

The University of Texas at Austin,

Le Laboratoire de physique des océans, Brest, France

with CNRS funded chair.

June 13, 2013

Outline

- Context: what drives abyssal diapycnal mixing? Not just IGWs in IGW band.
- Isolating wave and non-wave components.
- Data: Global Multi-Archive Current Meter Database.
- Properties of the non-wave components.

Abyssal mixing

- Central organizing theme of the theory of the general oceanic circulation is role of diapycnal mixing and the search for the conceptual model of how the microscale turbulence is maintained (*Munk and Wunsch*, 1998)
- What phenomena or mechanisms provide the energy?
- In most cases breaking internal gravity waves IGWs are implicated. "Whether generated by winds or tides, the breaking of internal waves is believed to be a principal contributor to pelagic turbulence" (*Munk and Wunsch*, 1998, p. 1998).
- The importance of IGWs in driving abyssal turbulence, and their dominance over non-wave motions with similar frequency has lead to considerable effort to characterize IGWs (see e.g.

Polzin and Lvov, 2011, and references therein).

- We find at least 15% to 20% (probably significantly more) of the energy of motions in the IGW band are *not* consistent with IGWs.
- This high-frequency non-wave motion is not geostrophically balanced, it should ultimately cascade to small and fast space-time scales that drive diapycnal mixing. Another important source of mixing.
- What are the properties of super-inertial *non*-IGW motions? How energetic? What origin? Instability mechanisms of mesoscale or submesoscale currents? Topographic origin?

Separating IGWs from non-IGWs

- Polarization relations between pressure p, velocity (u, v, w), density anomaly ρ.
- Horizontal velocity vector $\vec{V} = (u, v)$ rotates anticyclonically (*Gill*, 1982, Fig. 8.4).
- Summary of phase relationships for the Northern Hemisphere: The horizontal velocity vector rotates clockwise with increasing time, regardless of the direction of phase propagation, inscribing an ellipse. The ellipse is tilted in the direction of the major axis. If one rotates the axes so that u is along the major axis in the downward direction, and v along the minor axis, then the following phase relationships hold:
  - v and ρ are in phase

  - ρ lags w by $\pi/2$ (which was obvious because ρ anomalies are generated by vertical advection of the stable background density gradient).
  - u lags v by $\pi/2$ (which was obvious because of the CW rotation). And given the relations above, implies that u and w are always $\pi/2$ out of phase.

- The only phase relation that remains is that of p', and this is the one needed to determine the direction of phase and energy propagation. This is unfortunate since the pressure signal, while often measured, is completely dominated by the vertical motion of the instruments resulting from the tilting of the mooring. For upward propagating phase (downward energy propagation) p' is in phase with u. This is reversed for downward phase propagation. That is, for downward phase propagation the p' is in phase with w.

- Have fewer time series with collocated (u, v, T) that had less than 1 hr sampling and greater than 12 month duration. This means that Fofonoff's IGW consistent check (*Wunsch*, 1976) can be applied at fewer sites than the check of sense of rotation (anticyclonic for wave motion) of the horizontal current vector.

Data sources:

- GMACMD is a global collection of approximately 50,000 historical physical oceanographic time series, primarily derived from moored ocean current meter, temperature, and other *in situ* records obtained from diverse sources.
- Developed since 2006, and is one of the only efforts to consolidate all the available archives (see also (e.g. *Alford and Whitmont*, 2007)).
- Recent papers: (*Sen et al.*, 2008; *Arbic et al.*, 2009; *Scott et al.*, 2010; *Wright et al.*, 2012; *Timko et al.*, 2012; *Wright et al.*, 2013)
- GMACMD includes: Oregon State University Buoy Group Archive, several private collections and the following national

archives: National Ocean Data Center; Fisheries and Oceans, Canada; British Ocean Data Centre; Seismer, France; National Oceanography Institute, India; CSIRO, Australia; JODC, Japan, NIOZ, Netherlands; and archives from Italy and Spain ...

- Uniform format for easy access by standard MatLab routines, and uniformly quality controlled to form the largest database of such records.
- When possible compare nominal depth and pressure. If not, compare mean temperature against climatological temperature.
- Use time series correlations to confirm redundant records and to find errors in metadata such as latitude and longitude.
- Excluding shelf regions less than 250 m deep, there are over 5000 current meter records, 10,000 temperature records, and 4000 collocated measurement (u, v, T) records with less than

3 hr sampling and at least 6 months of good data. Reducing the sampling requirement to 1 hr has little effect but doubling the duration requirement about halves the numbers.

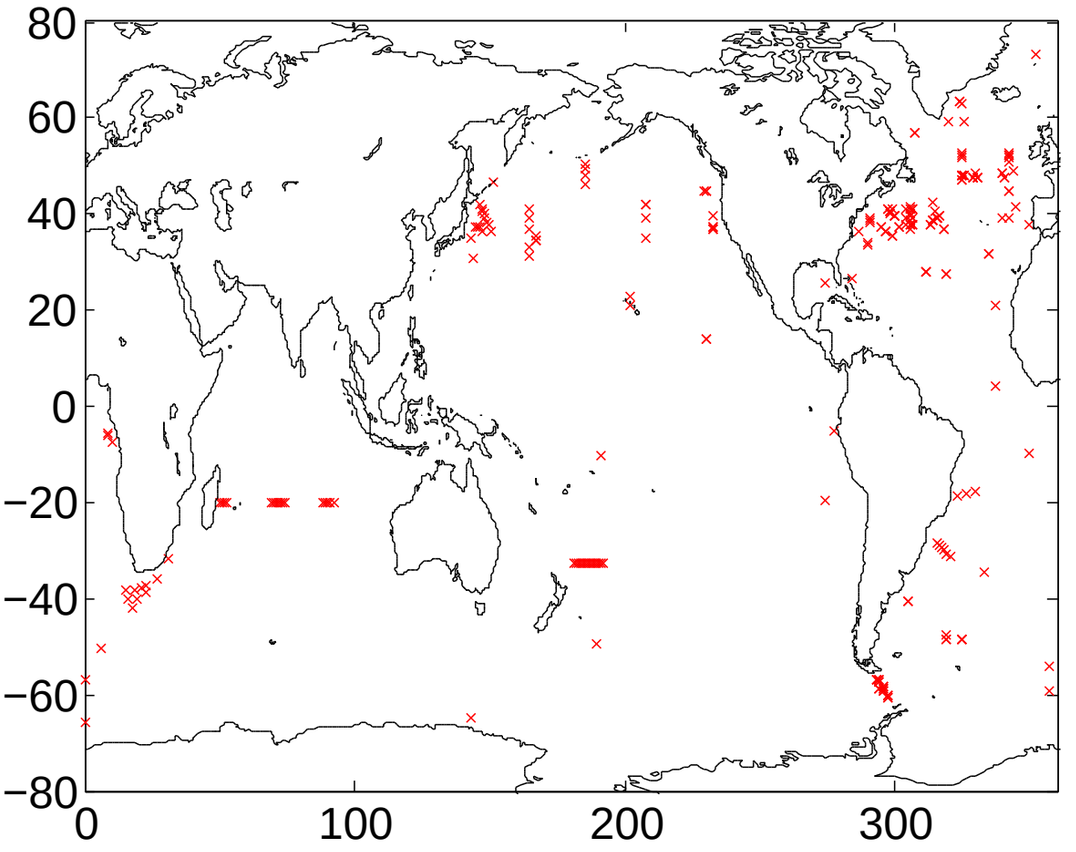

Figure 1: Location of 459 current meters: $\geq$ 12 months, $D \geq$ 2000 m, $\Delta t \leq 1$ hr

Rotary spectra

- Each time series reduced to 1-hour sampling rate.
- Rotary spectra applied to each time series
- Tides removed by interpolation over the points on either side of the M2 tidal peak.

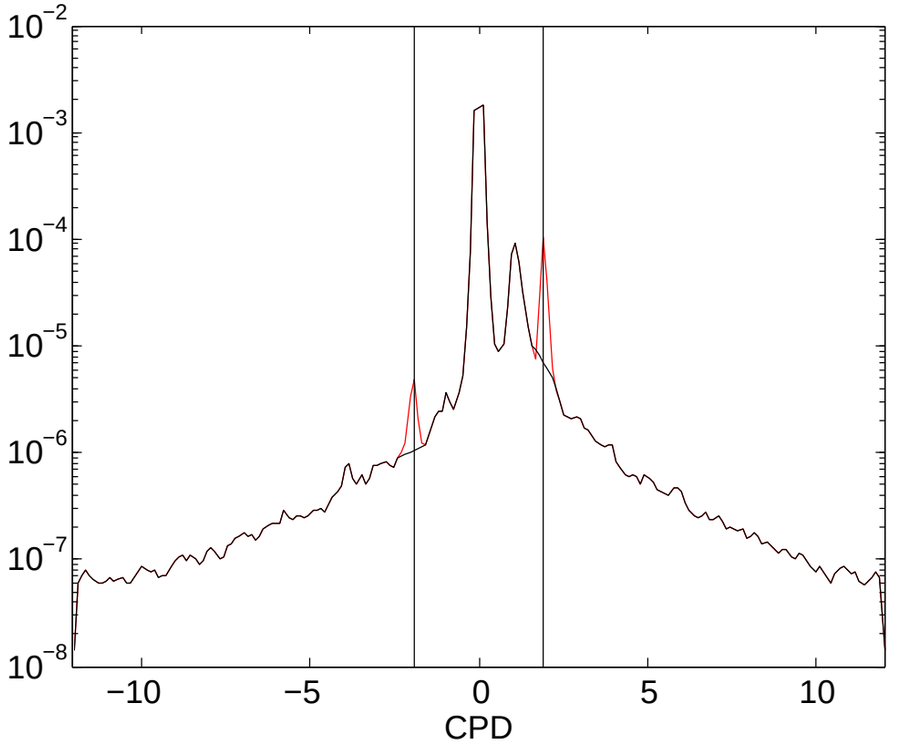

Figure 2: Rotary spectrum and tide removal

Integrals over IGW band

- Rotary spectra were integrated from the Nyquist frequency of -12 cycles per day (CPD) to $-0.9|f|$ to obtain the time series of KE in clockwise component (cyclonically rotating in the Southern Hemisphere), and similarly the integral from $0.9|f|$ to 12 CPD gave the anticlockwise component (anticyclonically rotating in the Southern Hemisphere).

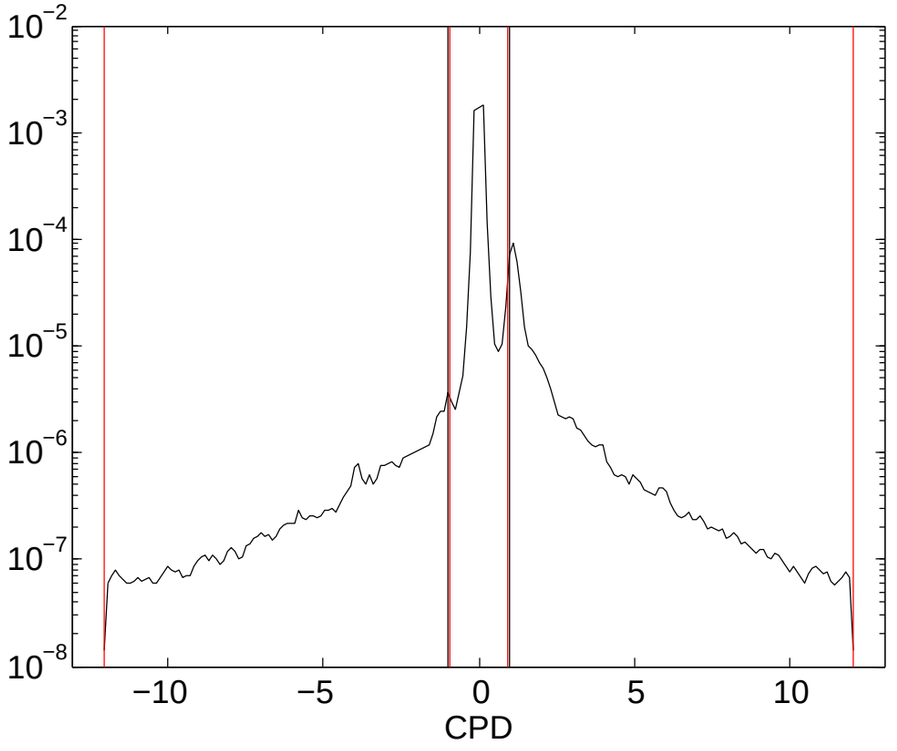

Figure 3: Rotary spectrum integrated from Nyquist to 10% beyond inertial frequency.

Fraction of energy in turbulent motions in IGW band

- At least 20% energy in deep ocean (within 1500 m of the seafloor) in super-inertial turbulence.
- At greater heights above the bottom, fraction falls gradually to about 10%.
- Similarly starting at the surface we find about 10% to 15% in the upper 2500 m.

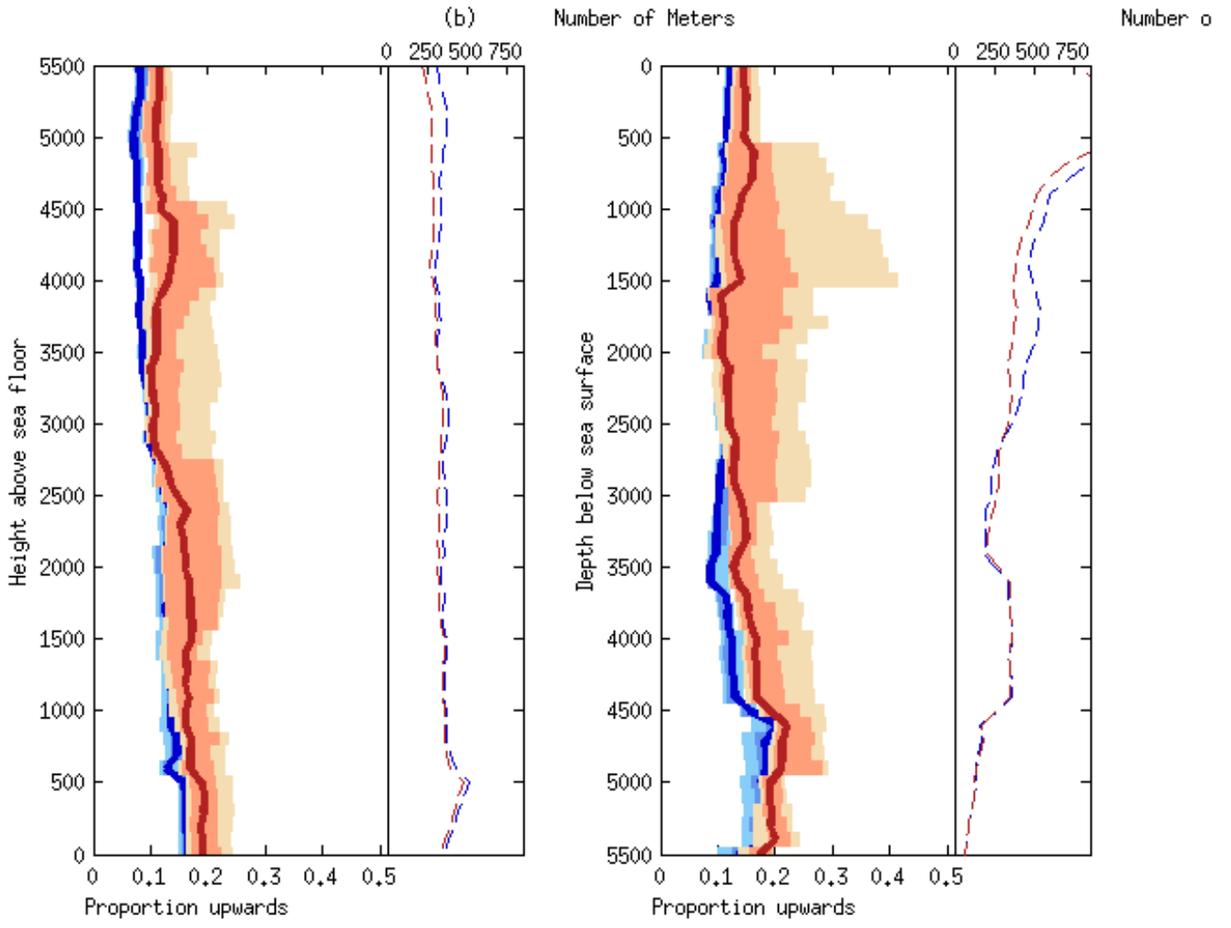

Figure 4: Fraction of energy with cyclonic rotation in the Northern Hemisphere (blue) and Southern Hemisphere (red)

Temporal correlation

- Want time series of the IGW band characteristics with time step of 15 days.
- We obtained rotary spectra from running 30-day windows, overlapping adjacent windows by 15 days.
- As before, the cyclonically rotating (turbulence) KE and anticyclonically rotating (IGW) KE obtained from integrating over the relevant parts of the rotary spectrum.
- Time series of mesoscale KE were obtained from simple running 30-day means.
- For each current meter record we obtained the Pearson correlation coefficient between KE in the IGW cyclonically (and anticyclonically) rotating component and the mesoscale KE.

Restrictions

Only used pairs of time series with/where:

- Where seafloor depth > 2000 m time series
- With at least 24 points, *i.e.* 360 days of overlapping 30-day windows. Assuming that we have only 10 degrees of freedom for the 24 points, the correlations greater than about 0.5 are statistically significant for a 1-sided test at the 95% level.

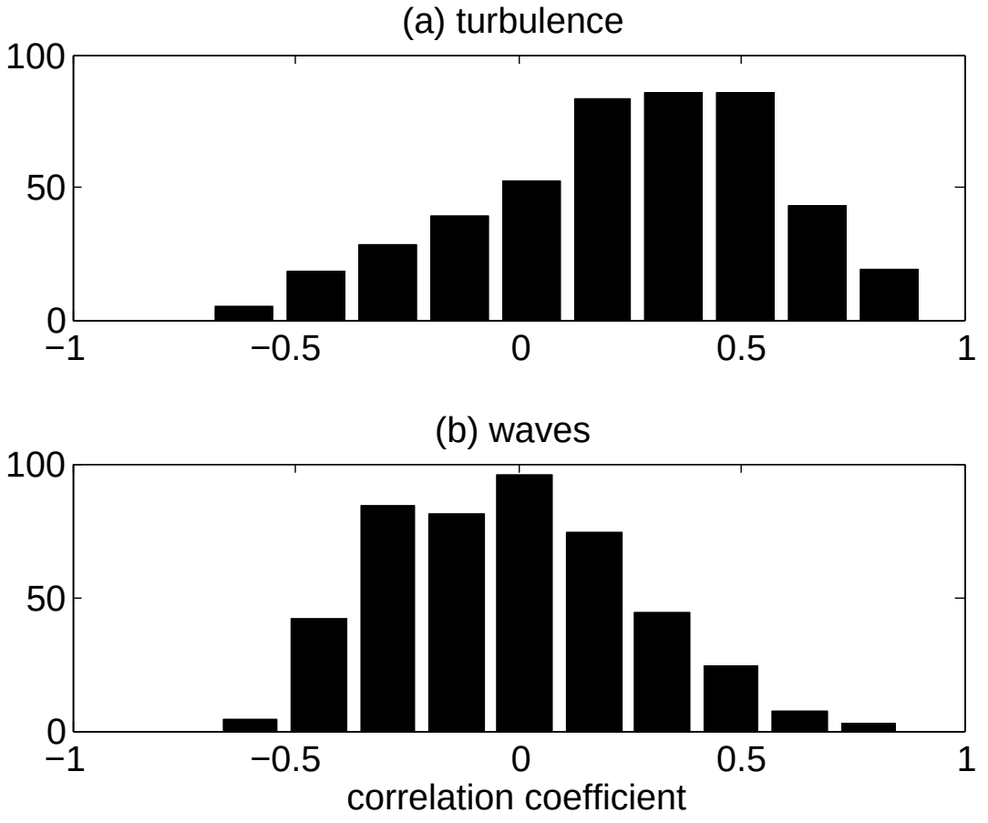

Figure 5: Histogram of the correlation coefficient between 459 time series of KE density in the IGW band and mesoscale EKE. (a) cyclonically rotating (non-waves) (b) anticyclonically rotating (possibly IGWs).)

Results: IGWs independent of mesoscale currents

- Only 15 records of 459 (or 3%) for the anticyclonically rotating component have correlation $r > 0.5$, which is less than what we would expect from chance alone (5%).
- Histogram appears to be almost symmetric about zero, supports zero correlation between IGWs and mesoscale KE.
- Consistent with the notion that the IGW component is wind-generated at the surface and unrelated to mesoscale currents.
- To check for the contamination from mooring blow-over, we repeated the analysis with 217 records that were within 2000 m of the bottom (still in at least 2000 m deep water), which

should minimize the blow-over effect (*Wunsch*, 1976). Almost identical results were found: Only 8 records of 217 (or 4%) for the anticyclonically rotating component have correlation $r > 0.5$.

Results: super-inertial turbulence modulated by mesoscale currents

- 109 records of 459 (24%) have correlation $r > 0.5$
- Histogram clearly asymmetric about zero, suggests relation between super-inertial turbulence and mesoscale KE.
- Consistent with the notion that in some locations the current meters are situated close to hotspots of wake turbulence driven by abyssal currents that generate cyclonically rotating non-waves in the IGW band.
- Repeated the analysis with 217 records that were within 2000 m of the bottom
- 48 records of 217 (22%) have correlation $r > 0.5$.

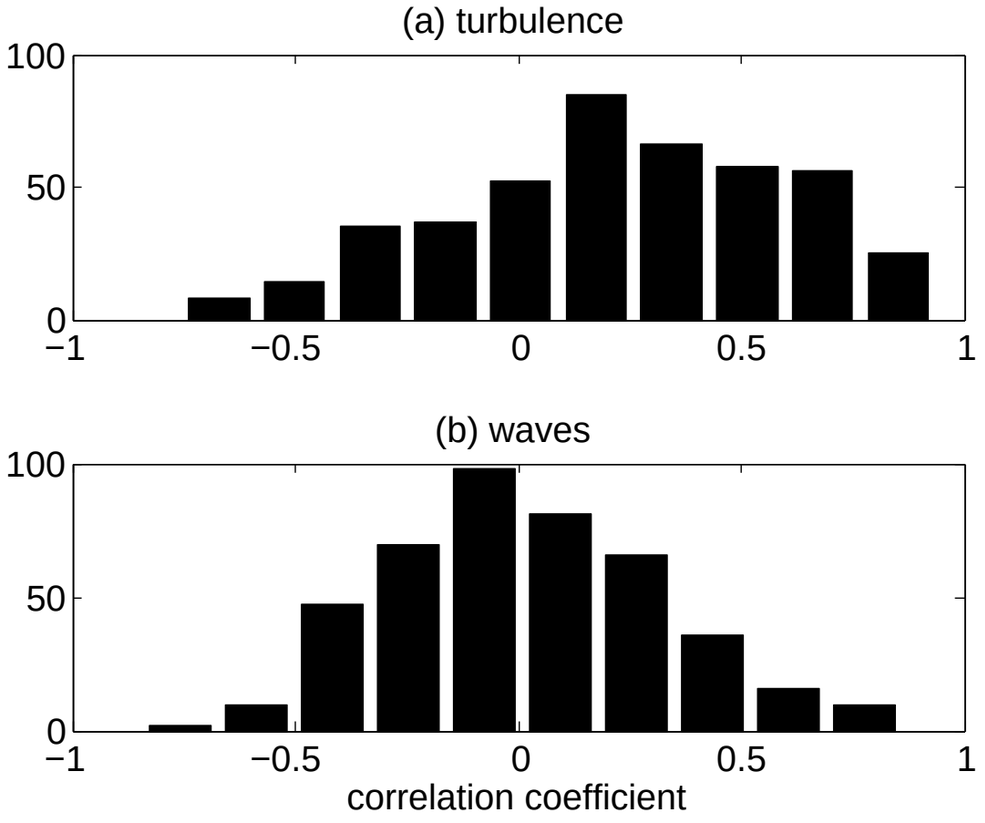

Figure 6: As before, but only for the 217 current meters within 2000 m of the bottom.

Future work

- How much of the anticyclonically rotating component is consistent with IGW motion?
- What is the origin of the super-inertial turbulence?
- Is topographic interaction involved?
- Divide moorings into rough/smooth topography, repeat analysis.

References

Alford, M. H., and M. Whitmont (2007), Seasonal and spatial variability of near-inertial kinetic energy from historical moored velocity records, *J. Phys. Oceanogr.*, *37*(8), 2022–2037, doi:10.1175/JPO3106.1.

Arbic, B. K., et al. (2009), Estimates of bottom flows and bottom boundary layer dissipation of the oceanic general circulation from global high-resolution models, *J. Geophys. Res.*, *114*, C02,024, doi:10.1029/2008JC005072.

Gill, A. (1982), *Atmosphere-Ocean Dynamics*, *International Geophysics Series*, vol. 30, 662 pp., Academic Press Inc., London, San Diego, 662 + xv pp.

Munk, W., and C. Wunsch (1998), Abyssal recipes II. Energetics of tidal and wind mixing, *Deep-Sea Res.*, *45*, 1977–2010.

Polzin, K. L., and Y. V. Lvov (2011), Toward regional characterizations of the oceanic internal wavefield, *Rev. Geophys.*, *49*, doi:{10.1029/2010RG000329}.

Scott, R. B., B. K. Arbic, E. P. Chassignet, A. C. Coward, M. Maltrud, J. Merryfield, A. Srinivasan, and A. Varghese (2010), Total kinetic energy in three global eddying ocean circulation models and over 5000 current meter records, *Ocean Modelling*, *32*, doi:10.1016/j.ocemod.2010.01.005.

Sen, A., R. B. Scott, and B. K. Arbic (2008), Global energy dissipation rate of deep-ocean low-frequency flows by quadratic bottom boundary layer drag: Computations from current-meter data, *Geophys. Res. Lett.*, *35*, L09,606 doi:10.1029/2008GL033,407.

Timko, P. G., B. K. Arbic, J. G. Richman, R. B. Scott, E. J. Metzger, and A. J. Wallcraft (2012), Skill tests of

three-dimensional tidal currents in a global ocean model: a look at the North Atlantic, *J. Geophys. Res. Oceans*, *117*(C08014), doi:10.1029/2011JC007617.

Wright, C., R. B. Scott, B. K. Arbic, and D. G. Furnival (2012), Ocean-eddy dissipation estimates at the Atlantic zonal boundaries, *J. Geophys. Res. Oceans*, *117*, doi:10.1029/2011JC007702.

Wright, C., R. B. Scott, B. K. Arbic, and D. G. Furnival (2013), Global observations of ocean-bottom subinertial current dissipation, *J. Phys. Oceanogr.*, *43*, doi:10.1175/JPO-D-12-082.1.

Wunsch, C. (1976), Geographic variability of the internal wave field: a search for sources and sinks, *J. Phys. Oceanogr.*, *6*, 471–485.